Short Note

Trans-Catena-Poly[[(Bis-(μ-N,N'-Bis[(Pyridin-3-yl)Methyl]Ethanediamide))-Diaqua-Cadmium(II)] Bis(Nitrate) Tetrahydrate)]

Anna Caria , Enrico Podda , Carla Aragoni , Riccardo Lai , Anna Pintus , Massimiliano Arca *

Posted Date: 11 June 2024

doi: 10.20944/preprints202406.0709.v1

Keywords: oxalamide; oxalic acid derivatives; hydrogen bonding; Cd; XRD; DFT

Short Note

Trans-Catena-Poly[[(Bis-(μ-*N,N'*-Bis[(Pyridin-3-yl)Methyl]Ethanediamide))-Diaqua-Cadmium(II)] Bis(Nitrate) Tetrahydrate)]

Anna Caria [1], Enrico Podda [1,2], M. Carla Aragoni [1], Riccardo Lai [1], Anna Pintus [1] and Massimiliano Arca [1,*]

[1] Dipartimento di Scienze Chimiche e Geologiche, Università degli Studi di Cagliari, S.S. 554 bivio Sestu, Monserrato, 09042 Cagliari, Italy
[2] Centro Servizi di Ateneo per la Ricerca (CeSAR), Università degli Studi di Cagliari, S.S. 554 bivio Sestu, Monserrato, 09042 Cagliari, Italy
* Correspondence: marca@unica.it

Abstract: The reaction between cadmium nitrate tetrahydrate and *N,N'*-bis(pyridin-3-ylmethyl)oxalamide (**L**) in 1:3 molar ratio in water/acetonitrile (1:6 v/v) mixture afforded single crystals of compound **1** suitable for X-ray diffraction analysis. Compound **1** consists of the coordination polymer (CP) $[[Cd(\mathbf{L})_2(H_2O)_2](NO_3)_2{\cdot}4H_2O]_\infty$, in which Cd^{II} ions are bridged by the neutral **L** antiperiplanar N-ligands in a wavy ribbon fashion developing along the *c*-axis. Two *trans*-disposed water molecules complete the *pseudo*-octahedral coordination geometry of the metal ion. The crystal packing of **1** revealed the interplay between π-π stacking interactions and an intricate hydrogen-bonded network involving oxalamides, nitrates and water molecules. The donor properties of **L** and the intermolecular interactions in compound **1** are interpreted based on hybrid-DFT calculations.

Keywords: oxalamide; oxalic acid derivatives; hydrogen bonding; Cd; XRD; DFT

1. Introduction

During the past decades, oxamic acid derivatives, i.e., oxalic acid monoamides, have encountered a flourishing interest due to the variety of their applications, ranging from medicine [1,2] to the conservation and restoration of cultural heritage [3–6]. Oxalyl diamides (oxalamides), i.e., oxalic acid diamides, have been widely employed in synthetic organic chemistry [7,8] and coordination chemistry [9,10]. In particular, *N,N'*-bis(pyridin-3-ylmethyl)oxalamide (**L**) was isolated in two polymorphs [11], as a hydrate [12], and it was structurally characterized in about fifteen different cocrystals and about thirty coordination compounds, where the pyridine N-atoms were directly involved in the coordination of transition metal ions as varied as Cu^{II} [13], Zn^{II} [14], Ni^{II} [15], Ag^{I} [16], Au^{I} [17], Co^{II} [18,19], and Pd^{II} [20]. In addition, four Cd^{II} complexes bearing the **L** oxalamide ligand in combination with carboxylate and dithiophosphato ancillary ligands have been reported to date [18,21].

We report here on the synthesis and the spectroscopic and structural solid-state characterization of the the coordination polymer (CP) $[Cd(\mathbf{L})_2(H_2O)_2](NO_3)_2{\cdot}4H_2O]_\infty$.

2. Results

N,N'-bis(pyridin-3-ylmethyl)oxalamide (**L**) was prepared in quantitative yield by refluxing pyridin-3-ylmethylamine and diethyloxalate in 2:1 molar ratio in water solution [6,16]. Crystals of compound **1** were grown by slow evaporation of an acetonitrile/water mixture of **L** and $Cd(NO_3)_2{\cdot}4H_2O$ in a 1:3 molar ratio (Scheme 1; Tables S1–S4). Compound **1** was characterized by elemental analysis, melting point determination, and FT-IR spectroscopy. Single crystal X-ray

 doi:10.20944/preprints202406.0709.v1

diffraction analysis established **1** as $[Cd(\mathbf{L})_2(OH_2)_2](NO_3)_2{\cdot}4H_2O$, crystallized in the triclinic space group $P\bar{1}$ (Figure 1).

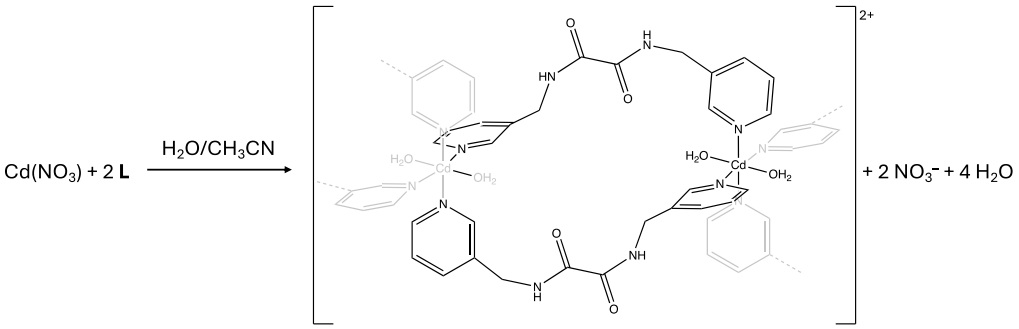

Scheme 1. Preparation scheme of $Cd(\mathbf{L})_2(OH_2)_2](NO_3)_2{\cdot}4H_2O$ (**1**) showing the connectivity in the resulting CP. The sketched grey fragments are shown for completeness, but are not included in the chemical balance.

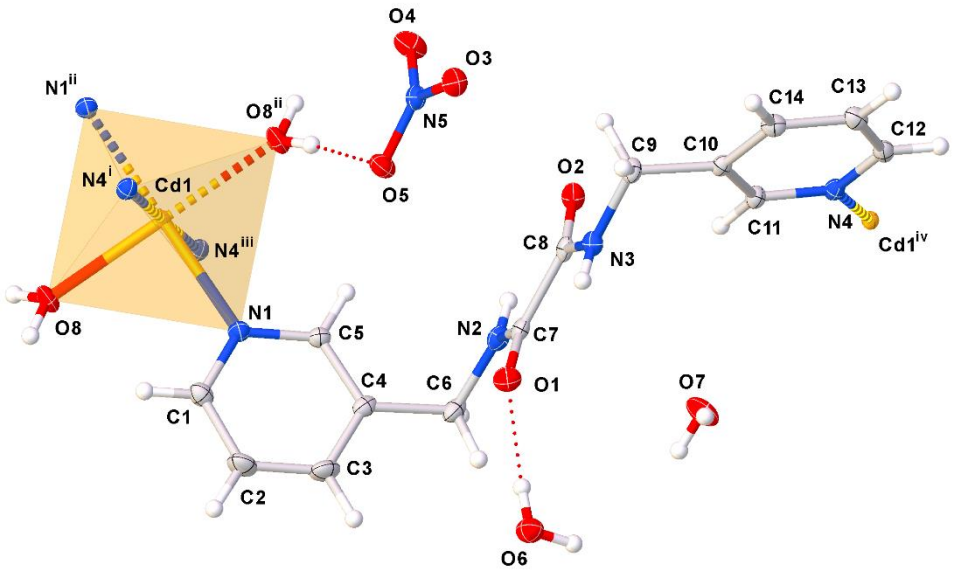

Figure 1. X-ray crystal structure of compound **1** with the numbering scheme adopted. Displacement ellipsoids were drawn at 50% probability level. The complete coordination sphere around the Cd^{II} ion is depicted showing symmetry-related atoms bonded through dashed bonds. Symmetry codes: ^{i} = $+x$, $+y$, $1+z$; ^{ii} = $1-x$, $1-y$, $2-z$; ^{iii} = $1-x$, $1-y$, $1-z$, ^{iv} = $+x$, $+y$, $-1+z$.

The asymmetric unit of compound **1** features a half-occupied Cd^{II} ion located on an inversion centre that is coordinated by a donor molecule **L** interacting through a pyridine N1 atom [Cd1–N1 = 2.3365(10) Å], a water molecule bound to the metal ion through the O8 atom [Cd1–O8 = 2.2991(9) Å], a nitrate and two co-crystallized water molecules. The **L** unit displays an antiperiplanar conformation of the oxalamide core with an O=C–C=O torsion angle of 174.7(1)° (Table S4), as previously found in the crystal structure determinations of different *N*,*N*′-dialkyloxalamides [22,23]. The C–C, C=O, and C–N bond lengths [1.533(1), 1.229(1)/1.233(1), and 1.325(1)/1.330(1) Å, respectively] are very close to the average values calculated for the 253 differently substituted free oxalamides deposited at the Cambridge Structural Database [CSD; average distances: C–C, 1.53(2); C–O, 1.23(1); C–N, 1.33(1) Å] [24]. Notably, all the 29 compounds containing **L** that were structurally characterized show the oxalamide in the same antiperiplanar conformation.

In the crystal structure of compound **1** each ligand unit bridges two symmetry-related Cd atoms (Cd and Cd^{iv} in Figure 1; Cd^{iv}–N4 = 2.3366(10) Å; ^{iv} = $+x$, $+y$, $-1+z$), so that each Cd atom shows a *pseudo*-octahedral coordination achieved by four N atoms lying on the meridian coordination plane

 doi:10.20944/preprints202406.0709.v1

and two *trans*-disposed water molecules. This coordination results in the formation of a CP featuring a ribbon-like motif propagating along the *c*-axis with Cd nodes shared between Cd_2**L**$_2$ links and self-complementary hydrogen bonds between oxalamides of adjacent **L** units forming a $R_2^2(10)$ motif (interaction *a* in Figures 2 and 3 and Table 1). In the crystal packing, adjacent ribbons are connected via face-to-face slipped π–π stacking interactions between pyridyl rings with distances between 3.70 and 3.82 Å, as shown in Figure 2b. The charge of the cationic ribbons is balanced by NO_3^- anions that, in combination with both coordinated and co-crystallized water molecules, define an intricate hydrogen bonded motif (interactions *b*-*h* in Figure 3 and Table 1).

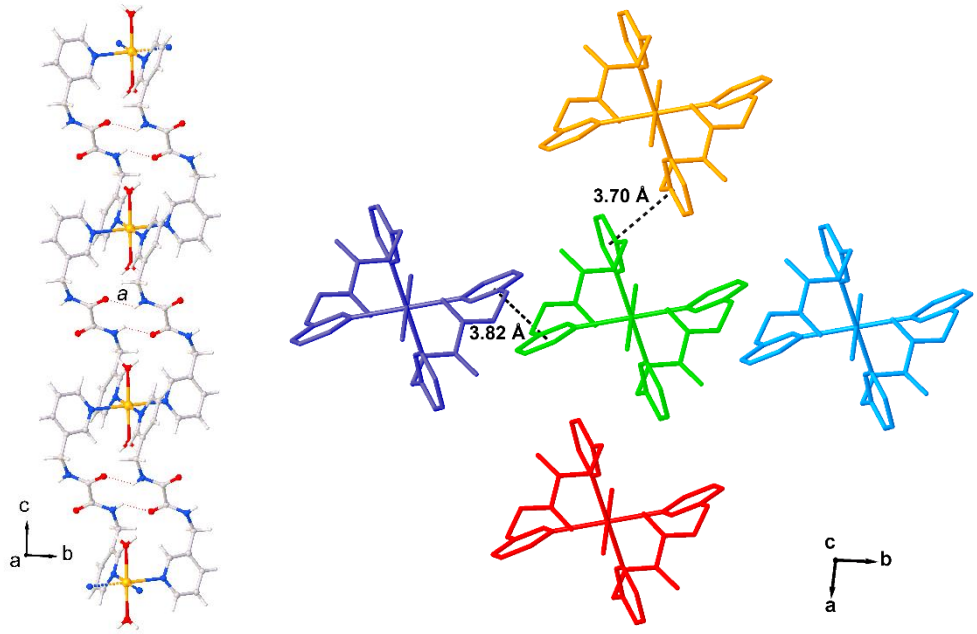

(**a**) (**b**)

Figure 2. Portion of the crystal packing of **1** showing: a) a single 1D-ribbon developing along the *c*-axis; b) the relative orientation of adjacent 1D-ribbons along the *c*-axis. Anions and co-crystallized water molecules were omitted for clarity. Interactions are labelled according to Table 1.

Table 1. Intermolecular interactions of compound **1**.

	Interaction A–B···C	$d_{A–B}$ (Å)	$d_{B\cdots C}$ (Å)	$d_{A\cdots C}$ (Å)	$\alpha_{A–B\cdots C}$ (°)
a	N2–H2···O2^{iii}	0.83(2)	2.159(2)	2.851(2)	140.7(2)
b	O6–H6C···O1	0.78(2)	2.039(2)	2.815(2)	172.0(2)
c	O8^{ii}–H8B^{ii}···O5	0.80(2)	1.98(2)	2.775(2)	177.8(2)
d	O6–H6D···O3^{v}	0.81(2)	2.08(2)	2.876(2)	166.2(2)
e	O8–H8A···O7^{i}	0.84(2)	1.84(2)	2.674(2)	175.7(2)
f	O7–H7A···O6^{vi}	0.81(2)	1.959(2)	2.765(2)	177.3(2)
g	N3^{v}–H3^{v}···O3^{vi}	0.82(2)	2.140(2)	2.937(2)	163.6(2)
h	O7–H7B···O4^{v}	0.80(2)	2.079(2)	2.872(2)	172.7(2)

Symmetry codes: ^{i} = +*x*, +*y*, 1+*z*; ^{ii} = 1−*x*, 1−*y*, 2−*z*; ^{iii} = 1−*x*, 1−*y*, 1−*z*; ^{v} = 1+*x*, +*y*, +*z*; ^{vi} = 2−*x*, 2−*y*, 1−*z*.

Preprints.org (www.preprints.org) | NOT PEER-REVIEWED | Posted: 11 June 2024 doi:10.20944/preprints202406.0709.v1

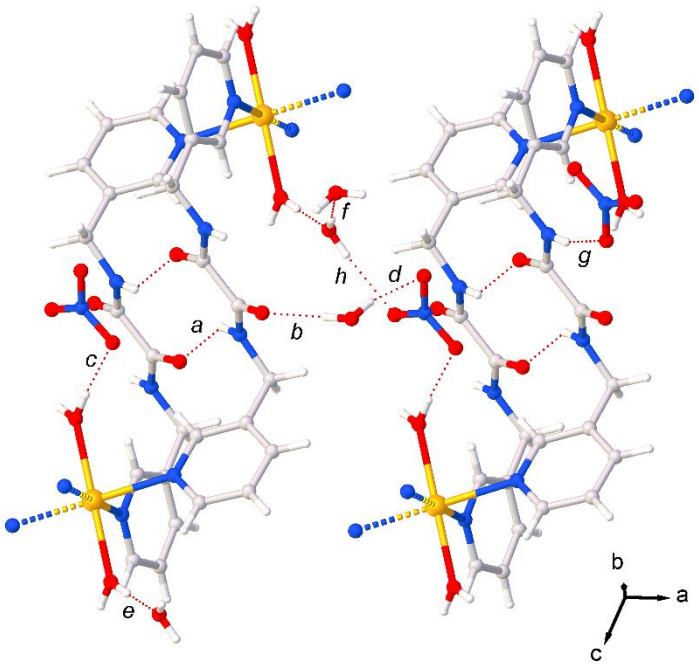

Figure 3. Hydrogen bonding network of **1** with interactions labelled according to Table 1.

A comparison between the solid-state FT-IR spectrum of compound **1** and that of the ligand **L** clearly shows the vibrational bands typical of C–H (2940–3050 cm^{-1}), N–H (3302 cm^{-1}), and C=O (1653–1655 cm^{-1}) stretching vibrations. A small but detectable shift in the C–N vibration of the pyridine ring was observed on passing from **L** to compound **1** (1525 and 1517 cm^{-1}, respectively) as a consequence of N-coordination (Figure S1). As expected, the broad band due to the O–H stretching mode of water molecules (3500 cm^{-1}) and those typical of the nitrate anion (1385 cm^{-1}) could only be envisaged in the FT-IR spectrum of compound **1**.

Finally, hybrid-DFT calculations shown that the lone pairs (LPs) of electrons on the pyridine nitrogen atoms of the ligand **L**, which feature remarkably negative natural charges (average charge Q_N = –0.481 |e|, Table S7), are available for coordination (Figure S2). Notably, the model complex cation $[Cd(\mathbf{L})_4(OH_2)_2]^{2+}$ was successfully optimized (Figure S3) and shown the same structural features as the complex unit in compound **1**. The terminal pyridine N-atoms in $[Cd(\mathbf{L})_4(OH_2)_2]^{2+}$ display natural charges ranging between –0.471 and –0.491 |e| (Table S8), demonstrating that the N-atoms on the terminal pyridine rings are available for further coordination and thus accounting for the formation of the CP in compound **1**.

3. Materials and Methods

3.1. General

All the reagents and solvents were used without further purification. *N,N′*-bis(pyridin-3-ylmethyl)oxalamide was synthesized as previously reported [16]. Fourier-Transform infrared (FT-IR) spectroscopic measurements were recorded at room temperature on a Thermo-Nicolet 5700 spectrometer on KBr pellets, with a KBr beam-splitter and KBr windows (4000–400 cm^{-1}; resolution 2 cm^{-1}). Melting point determinations were carried out on a FALC mod. C apparatus. DFT calculations were carried out both on **L** and the model compound $[Cd(\mathbf{L})_4(OH_2)_2]^{2+}$ at DFT level with the commercial suite of programs Gaussian 16 [25] by adopting the hybrid mPW1PW hybrid functional [26]. The def2SVP basis sets [27,28] were adopted for all the atomic species. Vibrational frequencies were calculated at the optimized geometries. BS data were extracted from the EMSL BS Library [29]. The memory required for each calculation was evaluated by the GaussMem cross-platform (Linux, macOS, Windows) program as a function of the number of shared processors, the total number of basis set functions, and a memory threshold depending on the highest angular momentum basis

 doi:10.20944/preprints202406.0709.v1

function [30,31]. Molecular geometry optimization for compound **1** was performed starting from structural data. Charge distributions were evaluated at the NBO level [32–34] at the optimized geometries. GaussView [35] was used to investigate the Kohn-Sham molecular orbital composition and charge distribution. X-ray diffraction data for compound **1** were collected at 100(2) K by means of ω scans with a Bruker D8 Venture diffractometer equipped with a PHOTON II area detector. Data reduction was carried out with SAINT v8.37[36] and SADABS-2016/2 [37] and the structure was solved with the ShelXT [38] solution program using dual methods. The model was refined by iterative cycles of least-squares refinement on F^2 ShelXL [39] 2018/3 and by using Olex2 1.5 [40] as the graphical interface.

Crystal data for compound **1**: $C_{28}H_{40}CdN_{10}O_{16}$, ($Mr$ = 885.10 g mol^{-1}) triclinic, *P -1* (No. 2), a = 9.1489(9) Å, b = 9.2546(9) Å, c = 11.6226(12) Å, α = 91.023(4)°, β = 112.441(4)°, γ = 93.497(4) °, V = 906.96(16) Å^3, T = 100(2) K, Z = 1, μ(Mo $K\alpha$) = 0.688 mm^{-1}, 44270 reflections measured, 4674 unique (R_{int} = 0.0390) which were used in all calculations. The final wR_2 was 0.0425 (all data) and R_1 was 0.0167 [$F^2 \geq 2\,\sigma(F^2)$].

*3.2. Synthesis of Compound **1***

To 3 mL of a CH_3CN solution of *N,N′*-bis(pyridin-3-ylmethyl)oxalamide (5.0×10^{-3} mol/L), a 1.0×10^{-1} mol/L solution of $Cd(NO_3)_2{\cdot}4H_2O$ in water was added (donor/Cd molar/ratio 1:3). A colourless crystalline precipitate formed in 24 h and was isolated from the mother liquor, gently washed with CH_3CN and air dried. A portion of the crystals was placed on a glass slide and coated with a perfluoroether oil. A crystal suitable for X-ray diffraction analysis was selected and mounted on a MiTeGen loop. M.p.: 232 °C. FT-MIR (KBr pellet, 4000–400 cm^{-1}): 3508w, 3288m, 3057vw, 2926vw, 2399vw, 2395vw, 1763vw, 1662s, 1606w, 1517m, 1452w, 1385vs, 1263w, 1236w, 1188vw, 1128vw, 1049vw, 985vw, 825m, 750vw, 696m, 648w, 511vw, 438vw, 407vw cm^{-1}.

4. Conclusions

Compound **1** was synthesized by the self-assembly of *N,N′*-bis(pyridin-3-ylmethyl)oxalamide and cadmium nitrate and its crystal structure elucidated by single crystal X-ray diffraction analysis. The crystal structure of compound **1** consists of a CP featuring cationic 1D-ribbons whose charge is counterbalanced by nitrate anions. Each Cd node shows a *pseudo*-octahedral coordination achieved by four pyridine N-atoms and two *trans*-disposed water molecules. The crystal packing results from the cooperation of π-π stacking interactions and hydrogen bonds involving oxalamides, water molecules and nitrates. Compound **1** confirms the potential of dipicolyloxalmides as flexible ligands for a variety of coordination compounds and opens new perspectives in the field of the crystal engineering of CPs and metal-organic frameworks.

Supplementary Materials: The following supporting information can be downloaded at: www.mdpi.com/xxx/s1; Figures S1: FT-IR; Figure S2 and S3: DFT optimized structures and Kohn-Sham molecular orbitals; Table S1: Crystal data and refinement parameters; Tables S2–S4: bond lengths, bond angles, and torsion angles; Table S5–S8: DFT-optimized geometries and natural charges.

Conceptualisation: MA, MCA. Data curation: MCA, EP. Investigation: AP, AC, RL. Writing (original draft): MA, EP. All authors have read and agreed to the published version of the manuscript.

Funding: The authors acknowledge the Ministero per l'Ambiente e la Sicurezza Energetica (MASE; formerly Ministero della Transizione Ecologica, MITE) – Direzione generale Economia Circolare for funding (RAEE – Edizione 2021). Fondazione di Sardegna (FdS Progetti Biennali di Ateneo, annualità 2022) is kindly acknowledged for financial support.

Data Availability Statement: Crystallographic data were deposited at the CCSD (CIF deposition number 2358751).

Acknowledgments: We acknowledge the CeSAR (Centro Servizi d'Ateneo per la Ricerca) of the University of Cagliari, Italy for providing access to the SC-XRD facility.

Conflicts of Interest: The authors declare no conflict of interest.

 doi:10.20944/preprints202406.0709.v1

References

1. Qiao, T.; Xiong, Y.; Feng, Y.; Guo, W.; Zhou, Y.; Zhao, J.; Jiang, T.; Shi, C.; Han, Y. Inhibition of LDH-A by Oxamate Enhances the Efficacy of Anti-PD-1 Treatment in an NSCLC Humanized Mouse Model. *Front. Oncol.* **2021**, *11*, 1033.
2. Miskimins, W.K.; Ahn, H.J.; Kim, J.Y.; Ryu, S.; Jung, Y.-S. Synergistic Anti-Cancer Effect of Phenformin and Oxamate. *PLoS ONE* **2014**, *9*, 85576.
3. Maiore, L.; Aragoni, M.C.; Carcangiu, G.; Cocco, O.; Isaia, F.; Lippolis, V.; Meloni, P.; Murru, A.; Slawin, A.M.Z.; Tuveri, E.; et al. Oxamate Salts as Novel Agents for the Restoration of Marble and Limestone Substrates: Case Study of Ammonium N-Phenyloxamate. *New J. Chem.* **2016**, *40*, 2768.
4. Pintus, A.; Aragoni, M.C.; Carcangiu, G.; Giacopetti, L.; Isaia, F.; Lippolis, V.; Maiore, L.; Meloni, P.; Arca, M. Density Functional Theory Modelling of Protective Agents for Carbonate Stones: A Case Study of Oxalate and Oxamate Inorganic Salts. *New J. Chem.* **2018**, *42*, 11593.
5. Maiore, L.; Aragoni, M.C.; Carcangiu, G.; Cocco, O.; Isaia, F.; Lippolis, V.; Meloni, P.; Murru, A.; Tuveri, E.; Arca, M. Synthesis, Characterization and DFT-Modeling of Novel Agents for the Protection and Restoration of Historical Calcareous Stone Substrates. *J. Colloid Interface Sci.* **2015**, *448*, 320.
6. Pintus, A.; Aragoni, M. C.; Carcangiu, G.; Caria, V.; Coles, S. J.; Dodd, E.; Giacopetti, L.; Gimeno, D.; Lippolis, V.; Meloni, P.; Murgia, S.; Navarro Ezquerra, A.; Podda, E.; Urru, C.; Arca, M. Ammonium *N*-(pyridin-2-ylmethyl)oxamate (AmPicOxam): A Novel Precursor of Calcium Oxalate Coating for Carbonate Stone Substrates. *Molecules* **2023**, 28, 5768.
7. Dong, K.; Elangovan, S.; Sang, R.; Spannenberg, A.; Jackstell, R.; Junge, K.; Li, Y.; Beller, M. Selective Catalytic Two-Step Process for Ethylene Glycol from Carbon Monoxide. *Nat. Commun.* **2016**, *7*, 1.
8. Zou, Y.Q.; Zhou, Q.Q.; Diskin-Posner, Y.; Ben-David, Y.; Milstein, D. Synthesis of Oxalamides by Acceptorless Dehydrogenative Coupling of Ethylene Glycol and Amines and the Reverse Hydrogenation Catalyzed by Ruthenium. *Chem. Sci.* **2020**, *11*, 7188.
9. Chen, Z.; Jiang, Y.; Zhang, L.; Guo, Y.; Ma, D. Oxalic Diamides and Tert-Butoxide: Two Types of Ligands Enabling Practical Access to Alkyl Aryl Ethers via Cu-Catalyzed Coupling Reaction. *J. Am. Chem. Soc.* **2019**, *141*, 3541.
10. Braun, M.; Frank, W.; Reiss, G.J.; Ganter, C. An N-Heterocyclic Carbene Ligand with an Oxalamide Backbone. *Organometallics* **2010**, *29*, 4418.
11. Jotani, M. M.; Zukerman-Schpector, J.; Madureira, L. S.; Poplaukhin, P.; Arman, H. D.; Miller, T.; Tiekink, E. R. T. Structural, Hirshfeld surface and theoretical analysis of two conformational polymorphs of *N*,*N*′-bis(pyridin-3-ylmethyl)oxalamide. *Z. Krist. Cryst. Mater*. **2016**, 231, 415.
12. DeHaven, B. A.; Chen, A. L.; Shimizu, E. A.; Salpage, S. R.; Smith, M. D.; Shimizu, L. S. Interplay between Hydrogen and Halogen Bonding in Cocrystals of Dipyridinylmethyl Oxalamides and Tetrafluorodiiodobenzenes. *Cryst. Growth Des.* **2019**, *19*, 5776.
13. Zeng., Q; Li, M.; Wu, D.; Lei, S.; Liu, C.; Piao, L.; Yang, Y.; An, S.; Wang, C. Organic–Inorganic Hybrid Aligned by the Ligand−Ligand Hydrogen Bonds by Using Pyridyl-Substituted Oxalamides as the Building Blocks. *Cryst. Growth Des.* **2008**, *8*, 869.
14. Hu, J. -H.; Hsu, H. -H.; Chen, Y. -W.; Chen, W. -H.; Liu, S. -M. Zinc(II) coordination polymers with mixed ligands: Synthesis, structures and evaluation on metal sensing. *J. Mol. Struct.* **2023**, 1289, 135896.
15. Lee, W. -T.; Liao, T. -T.; Chen, J. -D. Nickel(II) Coordination Polymers Supported by Bis-pyridyl-bis-amide and Angular Dicarboxylate Ligands: Role of Ligand Flexibility in Iodine Adsorption. *Int. J. Mol. Sci*. **2022**, *23*, 3603.
16. Schauer, C. L.; Matwey, E.; Fowler, F. W.; Lauher, J. Controlled Spacing of Metal Atoms via Ligand Hydrogen Bonds. *J. Am. Chem. Soc*. **1997**, *119*, 10245.
17. Wheaton, C. A.; Puddephatt, R. J. Complexes of gold(I) with a chiral diphosphine and bis(pyridine) ligands: Isomeric macrocycles and a polymer. *Polyhedron* **2016**, *120*, 88.
18. Chen, W. -J.; Lee, C. -Y.; Huang, Y. -H.; Chen, J. D. Cd(II) and Co(II) coordination polymers constructed from *N*,*N*′-Bis(3-pyridylmethyl)oxalamide and 1,4-naphthalenedicarboxylic acid. *Polyhedron* **2022**, *223*, 115991.
19. Liao, T. -T.; Lin, S. -Y.; Chen, J. -D. Co(II) coordination polymers supported by a benzenetetracarboxylate and bis-pyridyl-bis-amides with different flexibilities. *CrystEngComm* **2023**, *25*, 1723.
20. Qin, Z.; Jennings, M. C.; Puddephatt, R. J. Self-Assembly in Palladium(II) and Platinum(II) Chemistry: The Biomimetic Approach. *Inorg. Chem.* **2003**, *42*, 1956.
21. Tan, Y. S.; Yeo, C. I.; Kwong, H. C.; Tiekink, E. R. T. Unusual {···HNC_2O···HC_nO}, n = 1 or 2, synthons predominate in the molecular packing of one-dimensional coordination polymers, {$Cd[S_2P(OR)_2]_2(^3LH_2)$}n, for R = Me and Et, but are precluded when R = i-Pr; $^3LH_2$ = *N*,*N*′-bis(3-pyridylmethyl)oxalamide. *CrystEngComm* **2022**, *24*, 2992.
22. Podda, E.; Dodd, E.; Arca, M.; Aragoni, M. C.; Lippolis, V.; Coles, S. J.; Pintus, A. *N*,*N*′-Dipropyloxamide. *Molbank*, **2024**, *2024*, M1753.

 doi:10.20944/preprints202406.0709.v1

23. Podda, E.; Dodd, E.; Arca, M.; Aragoni, M. C.; Lippolis, V.; Coles, S. J.; Pintus, A. *N,N'*-Dibutyloxamide. *Molbank*, **2023**, *2023*, M1677.
24. CSD. ConQuest Software, Version 2024.1.0; The Cambridge Crystallographic Data Centre: Cambridge, UK, 2024.
25. Gaussian 16 (rev. C.01), Frisch, M. J.; Trucks, G. W.; Schlegel, H. B.; Scuseria, G. E.; Robb, M. A.; Cheeseman, J. R.; Scalmani, G.; Barone, V.; Petersson, G. A.; Nakatsuji, H.; Li, X.; Caricato, M.; Marenich, A. V.; Bloino, J.; Janesko, B. G.; Gomperts, R.; Mennucci, B.; Hratchian, H. P.; Ortiz, J. V.; Izmaylov, A. F.; Sonnenberg, J. L.; Williams-Young, D.; Ding, F.; Lipparini, F.; Egidi, F.; Goings, J.; Peng, B.; Petrone, A.; Henderson, T.; Ranasinghe, D.; Zakrzewski, V. G.; Gao, J.; Rega, N.; Zheng, G.; Liang, W.; Hada, M.; Ehara, M.; Toyota, K.; Fukuda, R.; Hasegawa, J.; Ishida, M.; Nakajima, T.; Honda, Y.; Kitao, O.; Nakai, H.; Vreven, T.; Throssell, K.; Montgomery, J. A., Jr.; Peralta, J. E.; Ogliaro, F.; Bearpark, M. J.; Heyd, J. J.; Brothers, E. N.; Kudin, K. N.; Staroverov, V. N.; Keith, T. A.; Kobayashi, R.; Normand, J.; Raghavachari, K.; Rendell, A. P.; Burant, J. C.; Iyengar, S. S.; Tomasi, J.; Cossi, M.; Millam, J. M.; Klene, M.; Adamo, C.; Cammi, R.; Ochterski, J. W.; Martin, R. L.; Morokuma, K.; Farkas, O.; Foresman, J. B.; Fox, D. J. Gaussian, Inc., Wallingford CT, 2016.
26. Adamo, C.; Barone, V. Exchange functionals with improved long-range behavior and adiabatic connection methods without adjustable parameters: The mPW and mPW1PW models, *J. Chem. Phys.* **1998**, *108*, 664.
27. Weigend, F.; Ahlrichs, R. Balanced basis sets of split valence, triple zeta valence and quadruple zeta valence quality for H to Rn: Design and assessment of accuracy. *Phys. Chem. Chem. Phys*. **2005**, *7*, 3297.
28. Weigend, F. Accurate Coulomb-fitting basis sets for H to Rn, *Phys. Chem. Chem. Phys*. **2006**, *8*, 1057.
29. Pritchard, B. P.; Altarawy, D.; Didier, B.; Gibson, T. D.; Windus, T. L. New Basis Set Exchange: An Open, Up-to-Date Resource for the Molecular Sciences Community. *J. Chem. Inf. Model*. **2019**, *59*, 4814.
30. Aragoni, M. C.; Podda, E.; Chaudhari, S.; Bhasin, A. K. K.; Bhasin, K. K.; Coles, S. J.; Orton, J. B.; Isaia, F.; Lippolis, V.; Pintus, A.; Slawin, A. M. Z.; Woollins, J. D; Arca, M. An experimental and theoretical insight into I_2/Br_2 oxidation of bis(pyridin-2-yl)diselane and ditellane. *Chem. – Asian. J.* **2023**, *18*, e202300836.
31. Arca, M. GaussMem 2024, https://massimiliano-arca.itch.io/gaussmem.
32. Reed, A. E.; Weinstock, R. B.; Weinhold, F. Natural population analysis. *J. Chem. Phys*. **1985**, *83*, 735.
33. Reed, A. E.; Weinhold, F. Natural localized molecular orbitals. *J. Chem. Phys*. **1985**, *83*, 1736.
34. Reed, A. E.; Curtiss, L. A.; Weinhold, F. Intermolecular interactions from a natural bond orbital, donor-acceptor viewpoint. *Chem. Rev*. **1988**, *88*, 899.
35. GaussView, Version 6, Dennington, Roy; Keith, Todd A.; Millam, John M. Semichem Inc., Shawnee Mission, KS, 2016.
36. APEX3, SAINT, Bruker AXS Inc.: Madison (WI), USA, 2015.
37. SADABS, Bruker AXS Inc., Madison (WI), USA, 2016.
38. Sheldrick, G. M. SHELXT - Integrated Space-Group and Crystal-Structure Determination. *Acta Cryst.* **2015**, *A71*, 3.
39. Sheldrick, G. M. Crystal Structure Refinement with SHELXL. *Acta Cryst.* **2015**, *C71*, 3.
40. Dolomanov, O. v.; Bourhis, L. J.; Gildea, R. J.; Howard, J. A. K.; Puschmann, H. OLEX2: A Complete Structure Solution, Re-finement and Analysis Program. *J. Appl. Crystallogr.* **2009**, *42*, 339.